

UNCLASSIFIED

AD 274 360

*Reproduced
by the*

**ARMED SERVICES TECHNICAL INFORMATION AGENCY
ARLINGTON HALL STATION
ARLINGTON 12, VIRGINIA**



UNCLASSIFIED

NOTICE: When government or other drawings, specifications or other data are used for any purpose other than in connection with a definitely related government procurement operation, the U. S. Government thereby incurs no responsibility, nor any obligation whatsoever; and the fact that the Government may have formulated, furnished, or in any way supplied the said drawings, specifications, or other data is not to be regarded by implication or otherwise as in any manner licensing the holder or any other person or corporation, or conveying any rights or permission to manufacture, use or sell any patented invention that may in any way be related thereto.

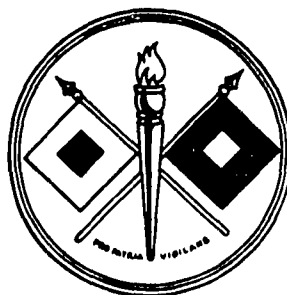
2743

by

**U. S. Army Signal Research and Development Laboratory
Fort Monmouth, New Jersey**

and

Hansjörg Oser
National Bureau of Standards
Washington, D. C.

**March 1962**

U. S. ARMY SIGNAL RESEARCH AND DEVELOPMENT LABORATORY
FORT MONMOUTH, NEW JERSEY

2411

U. S. ARMY SIGNAL RESEARCH AND DEVELOPMENT LABORATORY
FORT MONMOUTH, NEW JERSEY

March 1962

USASRD L Technical Report 2258 has been prepared under the supervision of the Director, Surveillance Department, and is published for the information and guidance of all concerned. Suggestions or criticisms relative to the form, contents, purpose, or use of this publication should be referred to the Commanding Officer, U. S. Army Signal Research and Development Laboratory, Fort Monmouth, New Jersey, Attn: Chief, Atmospheric Physics Branch, Meteorological Division.

J. M. KIMBROUGH, Jr.
Colonel, Signal Corps
Commanding

OFFICIAL:

H. W. KILLAM
Major, SigC
Adjutant

DISTRIBUTION:

Special

ASTIA Availability Notice

Qualified requesters may obtain copies of this report from ASTIA.

This report has been released to the Office of Technical Services, U. S. Department of Commerce, Washington 25, D. C., for sale to the general public.

March 1962

USASRDL Technical Report 2258

THEORETICAL CONSIDERATIONS
ON THE EFFECTIVENESS OF CARBON SEEDING

Robert Fenn
U. S. Army Signal Research and Development Laboratory
Fort Monmouth, New Jersey

and

Hansjörg Oser
National Bureau of Standards
Washington, D. C.

DA TASK NO. 3A99-27-005-03

U. S. ARMY SIGNAL RESEARCH AND DEVELOPMENT LABORATORY
FORT MONMOUTH, N. J.

ABSTRACT

Presented in the report are: some results of machine computations of the scattering functions, the extinction-, scattering-, and absorption-coefficients for pure absorbing carbon particles, and the compound carbon particles with concentric water shell of varying thickness; and an analysis of the absorption properties of various single particles.

The scattering and absorption properties of single particles are used to calculate the absorptivity, transmissivity, and reflectivity of three cloud models: a pure carbon particle cloud, a cloud of water droplets and carbon particles, and a cloud of compound concentric carbon-water particles. All three clouds are 1,000 meters thick and near the ground.

The temperature change of one particle caused by radiation absorption has been computed, and the total energy for evaporation of a cloud mass has been estimated.

From these calculations it can be concluded that a total carbon mass of the order of several hundred pounds per km^2 will be necessary to evaporate a stratus-type cloud.

CONTENTS

Abstract	i
INTRODUCTION	1
DISCUSSION	2
Absorption and Scattering Properties of Single Carbon and Carbon-Water Particles	2
Absorption of Radiation by Carbon Particles Suspended in the Atmosphere	15
CONCLUSIONS	24
REFERENCES	24

Figures

1. through 7.	Extinction-, scattering-, and absorption- coefficients for carbon particles of varying water shell thickness	4 through 7
8.	Absorption coefficient for constant total particle size as function of water shell thickness	9
9.	Total absorption cross section for const. b/a and increasing particle size	10
10. } 11. }	Absorption cross section for constant carbon nucleus size as function of water shell thickness	11
12. } 13. }	Scattering function for carbon particle with size parameter $\alpha = 0.6$ and 1	13
14.	Scattering function for water droplet and carbon particle with size parameter $\alpha = 50$	14
15.	Total absorption coefficient for a given total carbon mass per unit volume as a function of the size parameter	16
16.	Computed transmitted energy (E_D), absorbed energy (E_A) and reflected energy (E_R) for three cloud models, as function of sun zenith distance	19

Table

1.	Absorption coefficients for water droplets ($r = 6.265 \mu$) with carbon particles of $a = 0.171$, 0.215 , 0.368 and 0.480μ radius, and for pure water droplets	12
----	--	----

THEORETICAL CONSIDERATIONS ON THE EFFECTIVENESS OF CARBON SEEDING

INTRODUCTION

The first big step in artificial cloud modification was taken in 1946 when, through experiments conducted by Schaefer¹ and Vonnegut,² the artificial stimulation of precipitation from supercooled clouds became feasible. The technique applied by the two experimentalists was based on Findeisen's theory³ that in supercooled clouds the introduction of nuclei could initiate the formation of precipitation particles. Schaefer¹ found that small pieces of dry ice could form a large number of small ice crystals in such a cloud, and Vonnegut discovered that, also, tiny crystals of silver iodide would be very active as sublimation nuclei. Many successful seeding experiments with supercooled cumulus clouds as well as supercooled stratus clouds have since been carried out.

However, both of the above-mentioned seeding methods are confined to the application for supercooled clouds only, whose temperature is below 0°C; and all attempts to find a reliable method for the dissipation of warm clouds and fogs have been unsuccessful. The principal difficulty with warm-cloud seeding is that there is no "latent energy" in the cloud available which, after liberation, could carry on the dissipation process by itself.

In the case of supercooled clouds, this latent energy is the energy of fusion which becomes free after seeding and which has been provided in an indirect way by the decrease of the entropy of the system by nature itself. Whatever energy for a precipitation process or evaporation process is needed in a warm cloud, therefore, has to be fully supplied from an outside source. As such an energy source, the radiation energy from the sun is, of course, the most apparent. There are other forms of energy which could possibly be used; for instance, electrostatic forces for dissipation of fogs and clouds. These, however, will not be discussed in this report.

Using the properties of carbon-black particles suspended in the atmosphere, several attempts have been made to absorb and emit sunlight, thus influencing, artificially, the energy processes in the atmosphere and especially in clouds. In recent years, several investigators have made estimates of the energy absorbed in carbon spheres and clouds of carbon particles; and various hypotheses have been developed on the processes which might occur in carbon-seeded clouds. However, all these computations of the energy absorbed by carbon particles have been based on the so-called bulk method which uses the equivalent solid-mass layer for its absorption calculations, or they were based on very rough estimates of the absorption cross section. Such results, of course, may be considerably different from exact solutions of the formulas of the Mie theory.⁴

Actual carbon-seeding experiments have been carried out by Van Straten, Ruskin, Dinger, and Mastenbrook⁵ and by personnel of the Air Force Geophysics Research Directorate, but none of these experimental tests of carbon seeding gave a decisive answer to the question of the effectiveness of this method. It therefore seemed desirable to conduct some theoretical studies on the feasibility of carbon seeding, including an evaluation of the absorption properties of carbon-cloud elements according to the Mie theory⁴ and to find from this a sound basis for future experiments.

DISCUSSION

Absorption and Scattering Properties of Single Carbon and Carbon-Water Particles

As mentioned previously, for a comprehensive solution of the problem it is necessary to investigate the optical properties of pure carbon particles as well as compound carbon and water particles. The compound carbon-water particle, a carbon sphere with a concentric water shell around it, will be an idealization to some extent and will probably occur, in this form, only in the case of condensation of water around the carbon center. However, it is the only combination carbon-water droplet which can be treated theoretically. The exact formulas for such compound particles have been worked out by Aden and Kerker⁶ and are an extension of Mie's theory.⁴ They consider three different media separated by two boundary layers. With this theory, the absorption and scattering properties of pure spherical homogeneous particles with complex refractive index, and also of spherical particles with concentric shell of varying thickness can be computed. The following notations will be used:

- θ = Scattering angle ($\theta = 0$ is forward scattering)
- a = Radius of the inner sphere (carbon particle)
- b = Outer radius of the shell
- λ = Wavelength of the incident light
- m = $n(1 - n'i)$ = complex refractive index
- α = $2\pi a/\lambda$ = size parameter for a
- γ = $2\pi b/\lambda$ = size parameter for b
- b/a = Specific ratio.

According to Mie's theory and from Aden and Kerker's treatment,⁶ the following quantities are derived.

The cross sections for extinction and scattering,

$$Q_e = \frac{2}{\gamma^2} \sum_{n=1}^{\infty} (2n+1) \operatorname{Re}(a_n + b_n) \quad (1)$$

$$Q_s = \frac{2}{\gamma^2} \sum_{n=1}^{\infty} (2n+1) \cdot (|a_n|^2 + |b_n|^2). \quad (2)$$

The cross section for absorption,

$$Q_a = Q_e - Q_s. \quad (3)$$

The absolute intensities,

$$i_1 = |I_1|^2 \text{ and } i_2 = |I_2|^2 \quad (4)$$

$$\text{with } I_1 = \sum_{n=1}^{\infty} \frac{(2n+1)}{n(n+1)} \left\{ a_n \pi_n + b_n \tau_n \right\} \quad (5)$$

$$I_2 = \sum_{n=1}^{\infty} \frac{(2n+1)}{n(n+1)} \left\{ a_n \tau_n + b_n \pi_n \right\}. \quad (6)$$

The functions a_n and b_n depend on the refractive index and the size parameter(s); the π_n and τ_n are functions of the scattering angle only.

Numerical computations have been carried out for Q_e , Q_s , i_1 , and i_2 for pure carbon particles, refractive index $m = 1.59 - 0.66i$ ($b/a = 1$), and carbon spheres with a concentric water shell (b/a variable) for size parameter values ν from 0.1 to 200. The computations have been carried out under Signal Corps contract on the IBM 704 computer of the National Bureau of Standards, Washington, D. C.

In Figs. 1 through 7 the computed total extinction-, scattering-, and absorption-coefficients for compound water-carbon particles for various ratios b/a from 1 to 0 are plotted as functions of the size parameter. Since, per definition, the Q_e , Q_s , and Q_a give the ratio between an area with which a particle interferes with the incident light and the actual geometrical cross section, it can be seen that the effective absorption cross section of a pure carbon particle (Fig. 1) for $1 < a < 4$ becomes almost $1\frac{1}{2}$ its geometrical cross section. For $a < 0.5$ the extinction is practically due to absorption only, and for $a > 2$ scattering and absorption coefficients are of the same order of magnitude.

For absorbing particles, the Q -functions are very smooth and do not show the oscillations which are so characteristic for the extinction coefficient of nonabsorbing particles. However, as the thickness of the water shell around the carbon particle increases, more and more of the effect of the damping of the imaginary part of the refractive index is lost, and the oscillations in the Q -functions become stronger ($b/a = 1.1, 1.2, 1.5, 2, 5$ and 10 in Figs. 2 through 7, respectively) until for very large b/a ratios the Q -functions approach the values for pure water droplets.*

*The curves in Figs. 5 through 7 for values $\nu > 10$ do not contain enough computed points to identify them unambiguously. $Q_s(\nu)$ for $b/a = 10$ is practically already equal to $Q_s(\infty)$ for pure water.

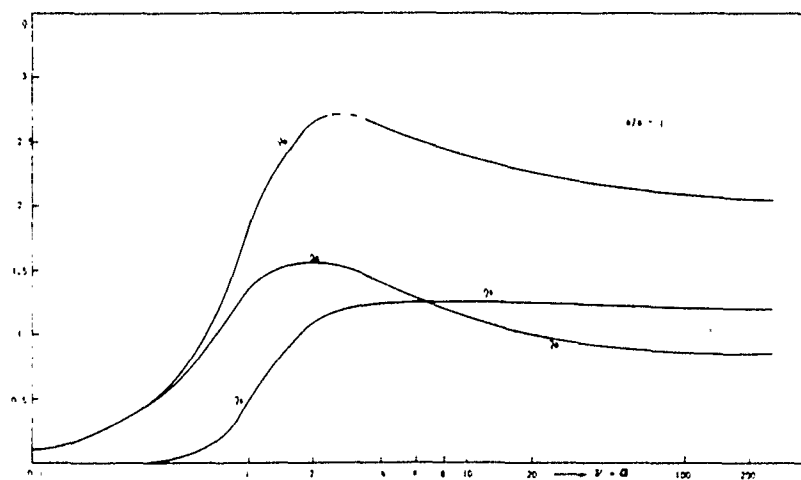


Fig. 1

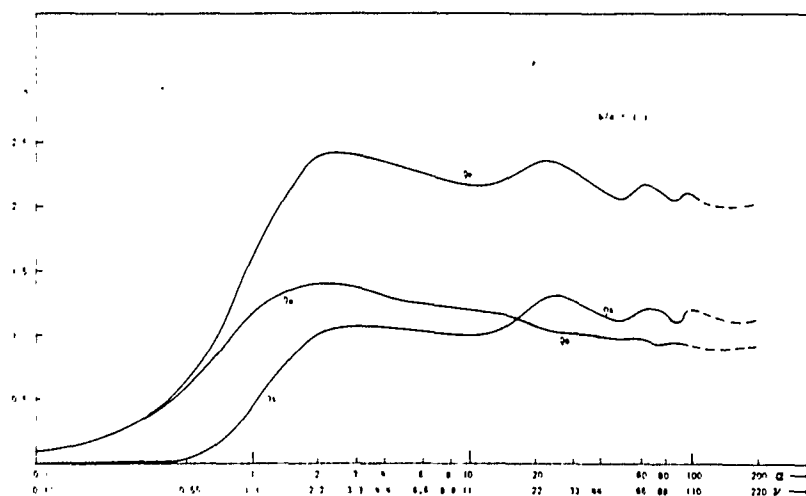


Fig. 2

Extinction-, scattering-, and absorption- coefficients
for carbon particles of varying water shell thickness.

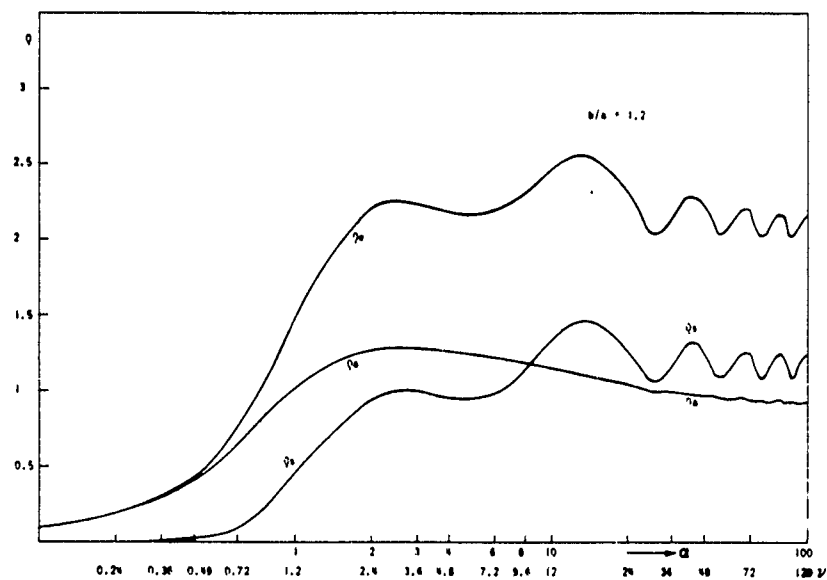


Fig. 3

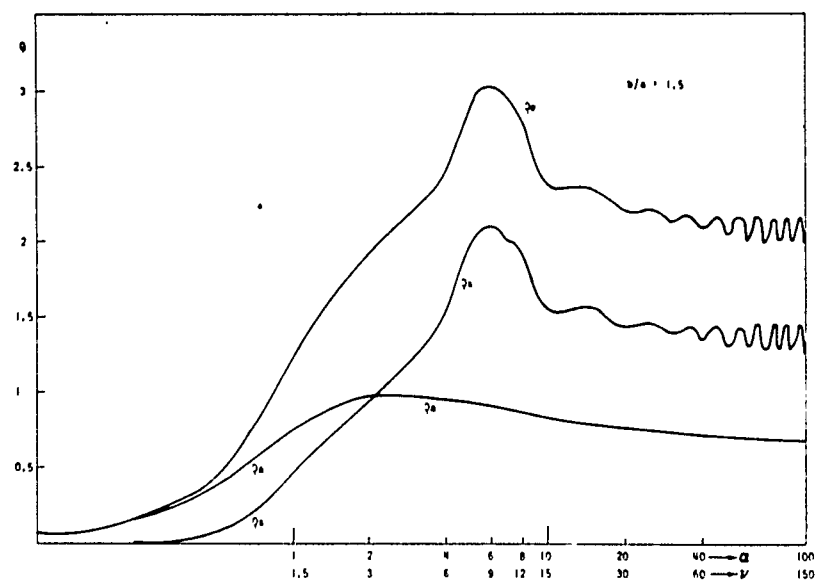


Fig. 4

Extinction-, scattering-, and absorption-coefficients
for carbon particles of varying water shell thickness.

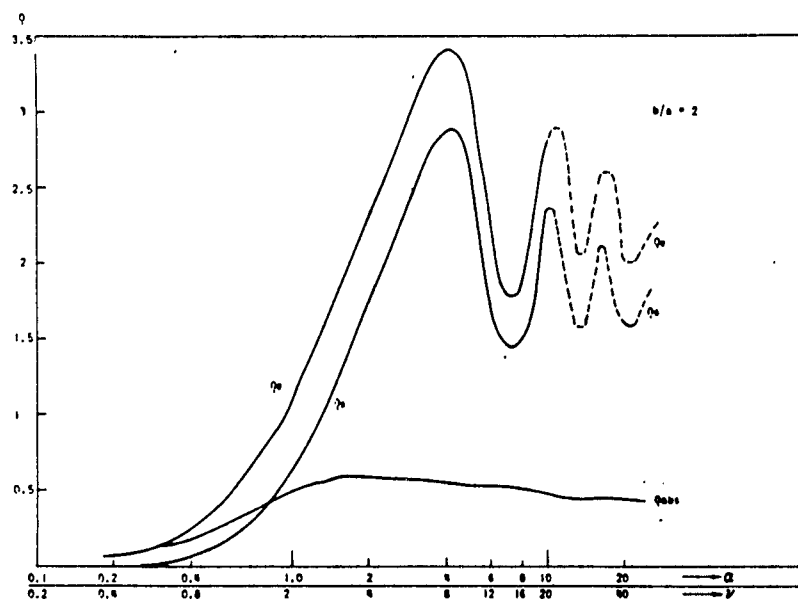


Fig. 5

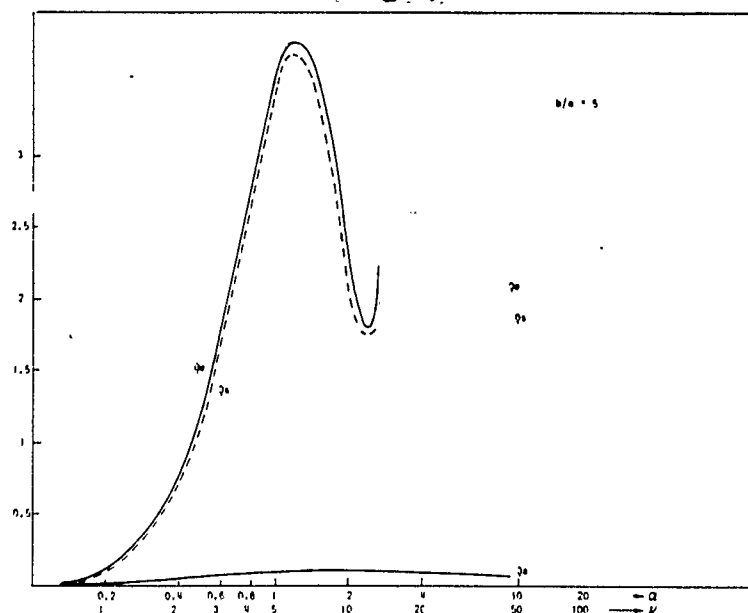


Fig. 6

Extinction-, scattering-, and absorption-coefficients for carbon particles of varying water shell thickness.

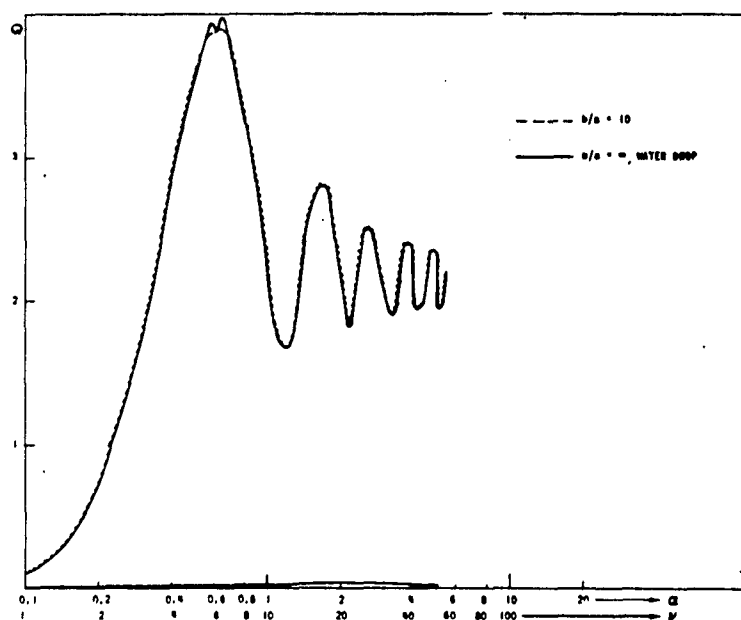


Fig. 7. Extinction-, scattering, and absorption-coefficients for carbon particles of varying water shell thickness.

In Fig. 8, the absorption coefficient Q_a (referring to a pure carbon particle as 100 percent), has been plotted as a function of b/a for constant total particle size ($\psi = \text{const}$). It can be seen from this graph that for larger particles ($\psi > 10$) the absorption coefficient of a carbon particle will be increased even by a thin water shell ($b/a = 1.1$). However, if b/a increases further, the water shell begins to reduce the absorption effect of the carbon nucleus. This shielding effect of the water shell is the stronger, the smaller the total particle size parameter.

According to the definition for Q_a , the absorption cross section of one particle is

$$C_a = r^2 \cdot \pi \cdot Q_a, \quad (7)$$

where r is the radius of the outer shell; i.e., in the case of compound particles, b is used instead of r . From this it follows that the absorption effect C_a of a compound particle which grows bigger and bigger disappears only if $Q_a(b)$ decreases more than b^2 increases with increasing b . However, since Q_a is a function of α and ψ , or of either α or ψ plus b/a , different results are obtained for equation (7), depending on whether b/a or ψ is kept constant. If α and ψ grow proportionally ($b/a = \text{const}$), the increase of b^2 will always be of higher order than the one for Q_a , and therefore $C_a \rightarrow \infty$ as ψ increases (Fig. 9). Whereas, if α is kept constant and the water is allowed to grow around the carbon particle (i.e., b/a variable), Q_a (ψ) will decrease much more for increasing ψ (Figs. 10 and 11). In Fig. 8 it is seen that even the efficiency factor for absorption Q_a itself increases above the one for a pure carbon particle if a thin water shell forms around the carbon core. In Figs. 10 and 11 for $\alpha = 0.1$ and $\alpha = 1$, the function $C_a = b^2 \pi \cdot Q_a(b/a)$ has been plotted. A normalizing factor C has been added, so that $C \cdot b^2 \cdot \pi \cdot Q_a(b/a = 1) = Q_a(b/a = 1)$, or since in this case $b^2 = a^2$, C becomes $1/a^2$, which is constant per definition. C_a increases to a peak value two to three times the C_a for a pure carbon particle, and then diminishes again. This means that the water skin acts in the direction to increase the absorption effect of the carbon particle. The absolute values decrease considerably if the size of the carbon particle itself gets smaller. Computations up to specific ratios b/a of 150 show that the absorption cross section $C_a = b^2 \pi \cdot Q_a$ remains finite and its obsolete value stays constant around the value for $C_a(b/a = 20)$.

An investigation was made of the wavelength dependence of the absorption coefficient of carbon particles. From Fig. 1 it can be seen that for $\alpha < 1.5$ and for $3 < \alpha < 20$ the absorption for carbon particles of constant size is wavelength dependent, and that for $\alpha < 1.5$ the absorption is the smaller, the larger the wavelength. The opposite is the case for $3 < \alpha < 20$. The range $\alpha < 1.5$ corresponds for visible light to very small particles ($r < 0.1 \mu$). Over the wavelength range $0.3 < \lambda < 0.7$, Q_a can vary by a factor 2. This results in the phenomena that industrial smoke quite often appears red-brown in the transmitted light if the particles are uniform enough in size and very small. As the particles become less absorbing (Figs. 2 through 7), the slope of Q_a becomes flatter and the wavelength dependence gradually disappears.

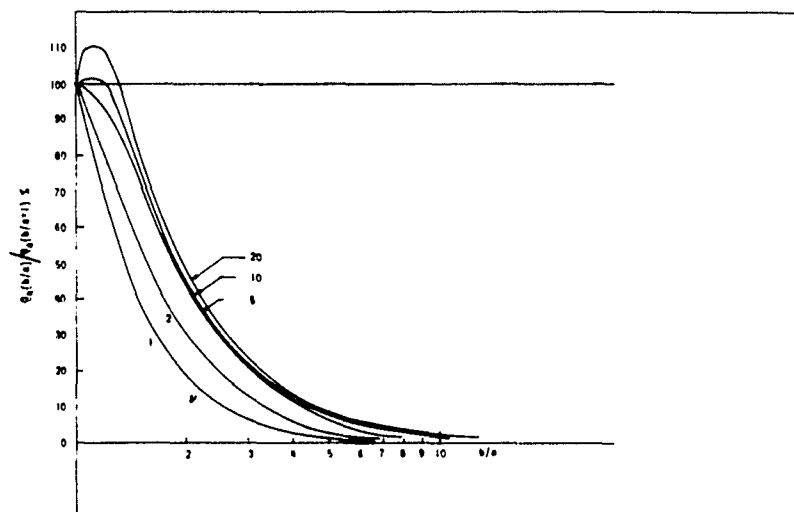


Fig. 8. Absorption coefficient for constant total particle size as function of water shell thickness.

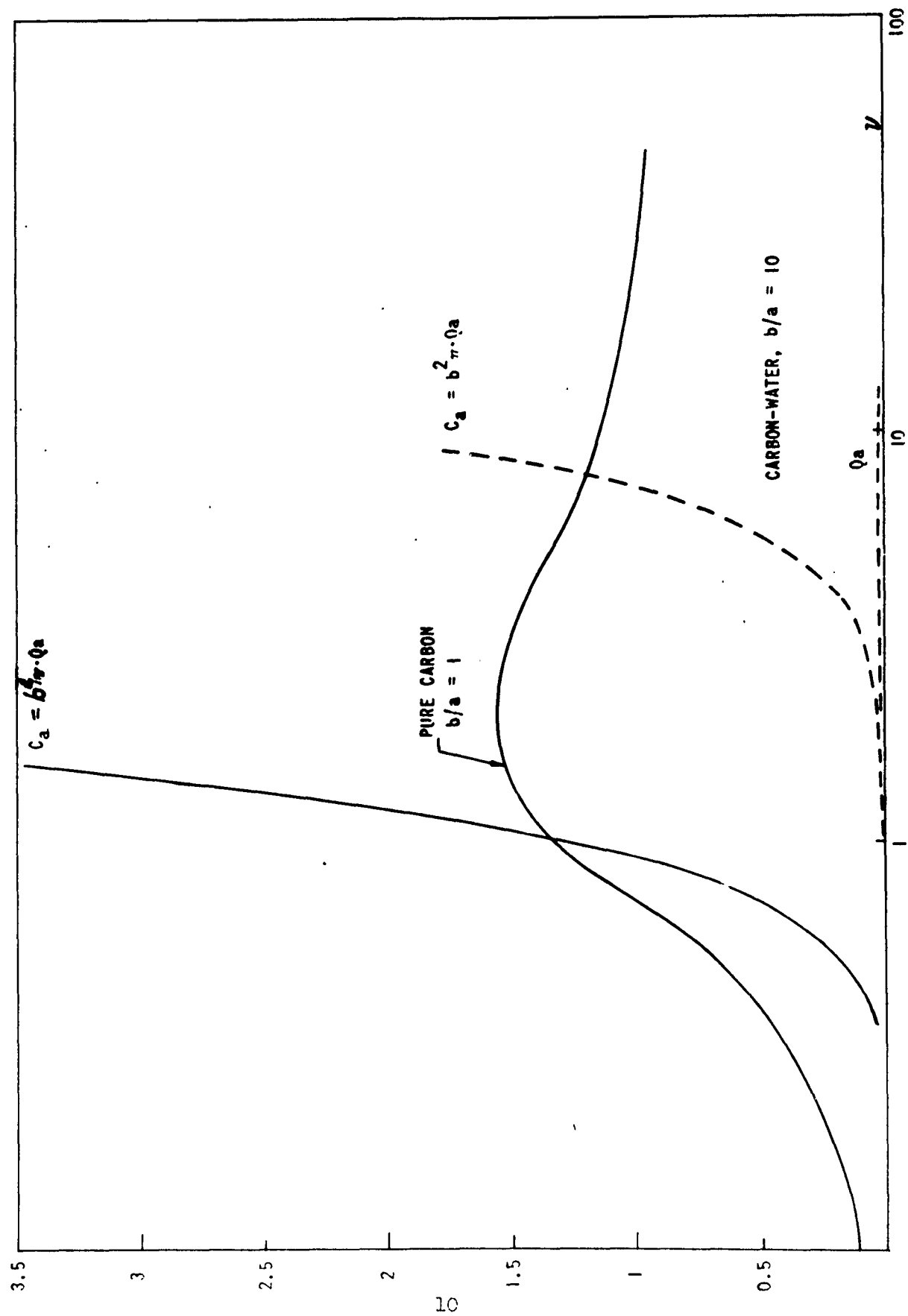


Fig. 9. Total absorption cross section for const. b/a and increasing particle size.

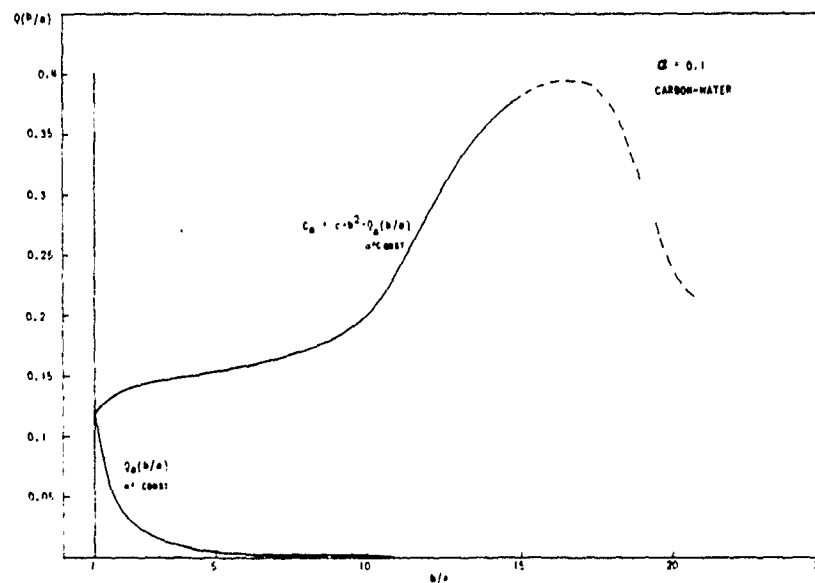


Fig. 10

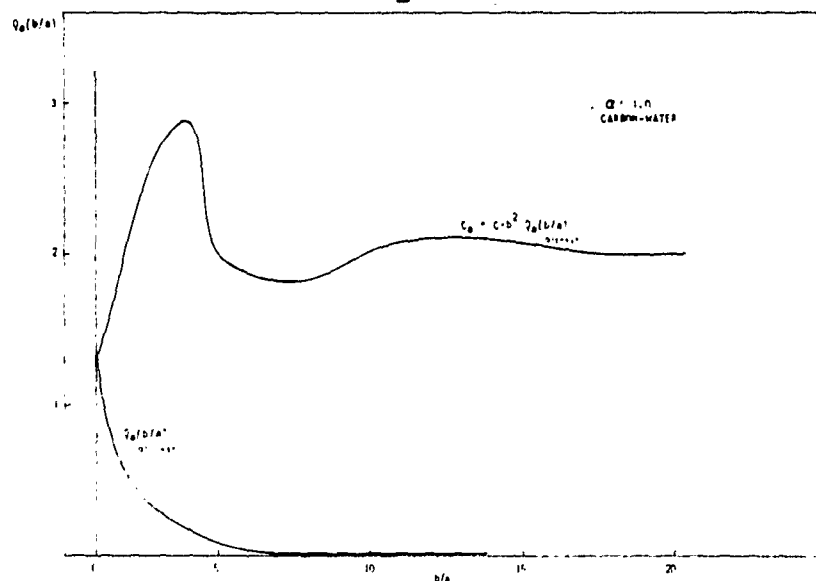


Fig. 11

Absorption cross section for constant carbon nucleus size as function of water shell thickness.

The influence of water absorption in the infrared region on the total absorption of compound carbon-water particles must also be studied. In Table 1 the computed Q_a are listed for a total particle size $b = 6.265 \mu$ (to be comparable with Shifrin's computations⁷) and for carbon-particle radii between $a = 0.171$ and 0.48μ for wavelengths from 1.35 to 10 microns. The absorption data for water in these computations have been taken from Dietrich⁸ and Shifrin.⁷ It can be seen that the contribution of the carbon particle to the total Q_a decreases with increasing specific ratio b/a , and if b/a is larger than about 10, only about 10 percent of the total absorption will be due to the carbon nucleus. In other words, with respect to absorption properties, a compound carbon-water particle with large b/a can be treated in the infrared like a pure water droplet without introducing a large error.

Table 1. Absorption coefficients for water droplets ($r = 6.265 \mu$) with carbon particles of $a = 0.171, 0.215, 0.368$ and 0.480μ radius, and for pure water droplets.*

$\lambda (\mu)$	Q_a , water and carbon				Q_a , pure water
	$b/a = 36.6$ $a = 0.171$	$b/a = 29.1$ $a = 0.215$	$b/a = 17$ $a = 0.368$	$b/a = 13.5$ $a = 0.480$	$b/a = \infty$
1.35	0.0051	0.0062	0.0121	0.0171	
1.5	0.0427	0.0440	0.0493	0.0537	
2.0	0.0790	0.0798	0.0851	0.0895	
3.0	1.1846	1.1846	1.1846	1.1846	0.894
3.2	1.1910	1.1910	1.1910	1.1910	
3.4	1.0143	1.0144	1.0153	1.0162	0.925
4.5	0.5004	0.5005	0.5022	0.5045	0.500
5.47	0.3716	0.3719	0.3734	0.3754	
6.0	1.1311	1.1311	1.1312	1.1313	1.127
7.0	0.7374	0.7376	0.7384	0.7395	0.704
10.0	0.5751	0.5753	0.5757	0.5763	0.575

In Figs. 12 through 14 the scattering functions have been plotted for a pure carbon particle for $\alpha = 0.6$ and $\alpha = 1$ and also $\alpha = 50$. As a comparison, the scattering function for a pure water droplet of the same size has been added. It can be seen that the angular distribution of the scattered light for small α -values depends only slightly on the refractive index. However, the total amount of scattered light is larger for carbon than for water particles. The scattering function for large-size parameter values is particularly interesting since, until recently, no exact computations for large α -values were available. With increasing α , the convergence of the infinite series of the a_n and b_n becomes very poor, and more and more terms have to be computed. In addition, the number of oscillations in the i_1 and i_2 increases proportionally to α . As Van DeHulst⁹ has shown, the

*Values for water droplets ($r = 6.265 \mu$) taken from Shifrin.⁷

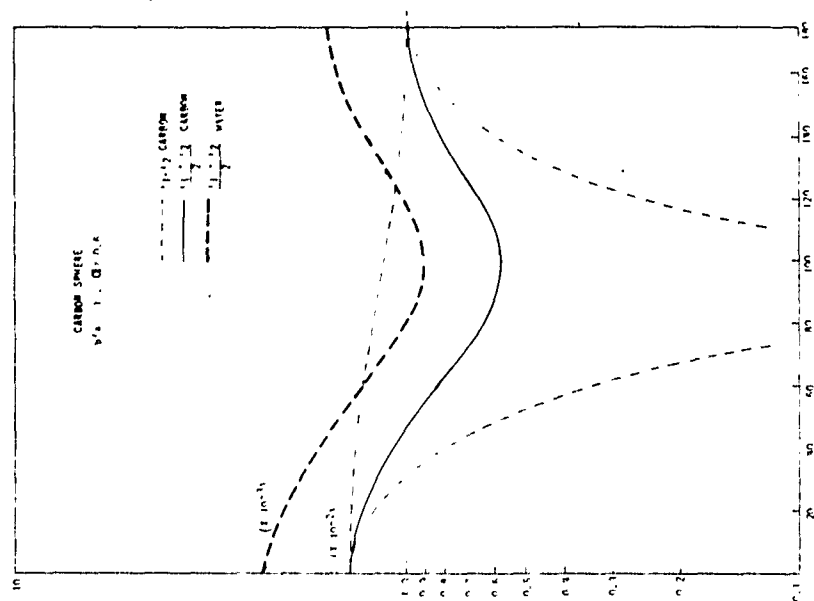


Fig. 12

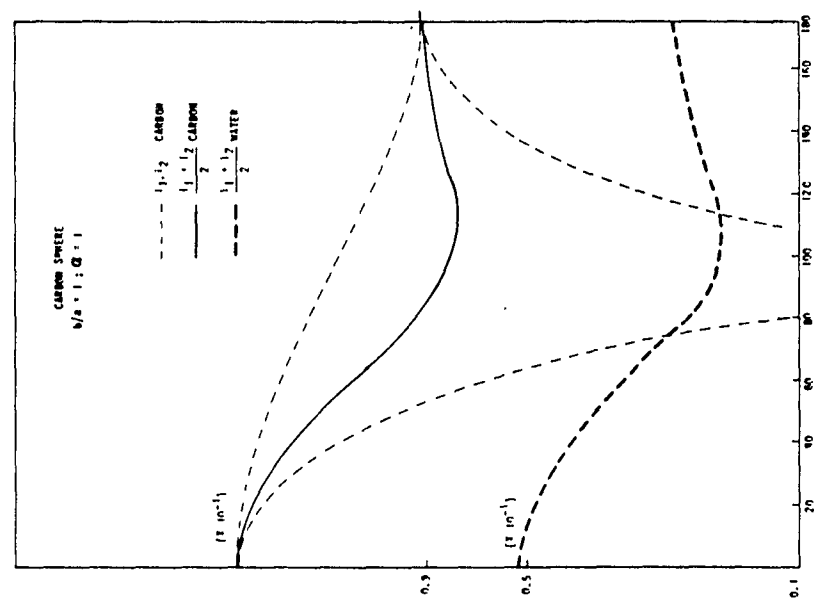
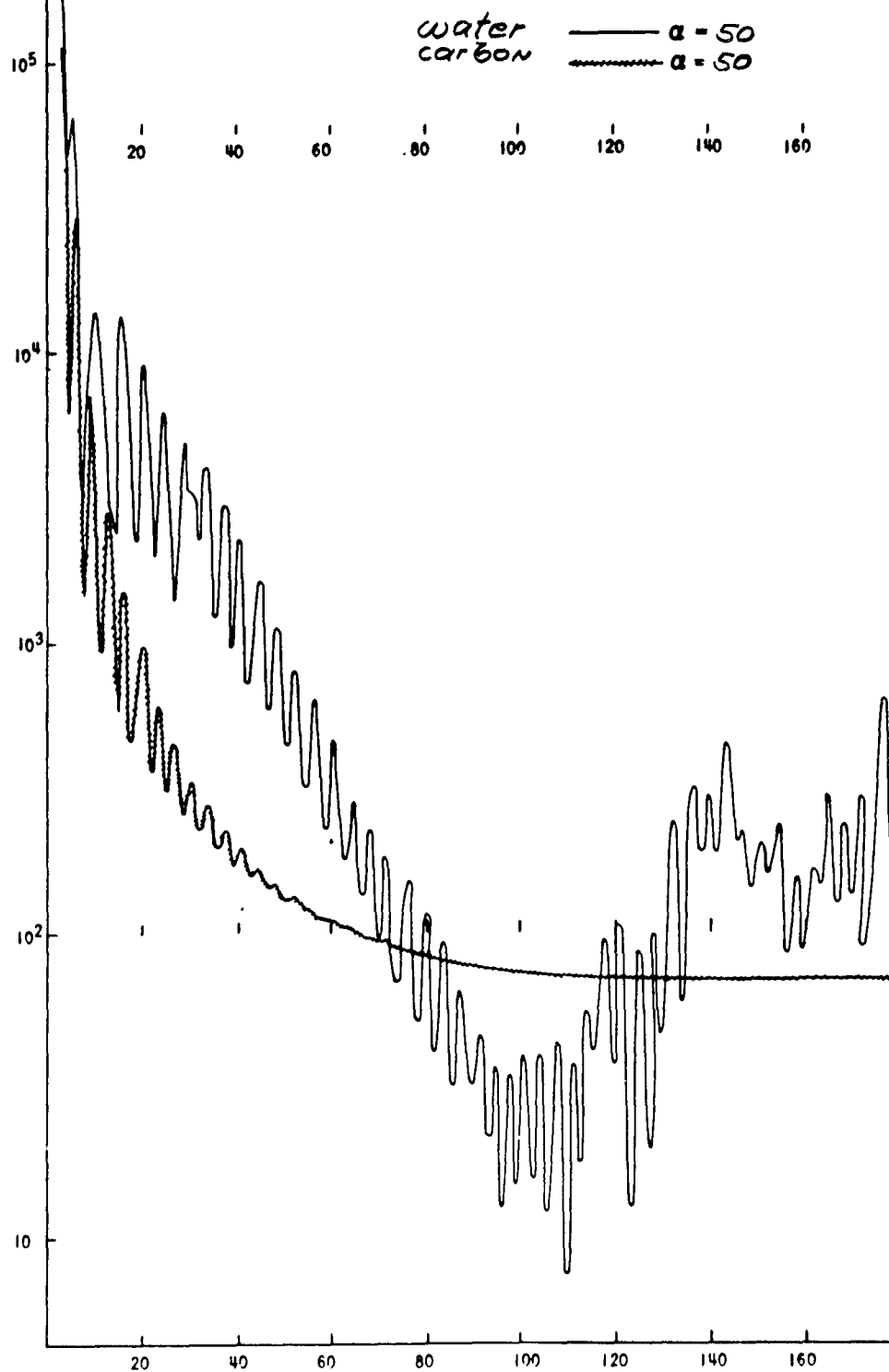


Fig. 13

Scattering function for carbon particle with size parameter $\alpha = 0.6$ and 1 .

Fig. 14. Scattering function for water droplet and carbon particle with size parameter $\alpha = 50$.



distance between two consecutive maxima becomes approximately $180^\circ/\alpha$. This has been proved by computations of Giese¹⁰ for water drops ($\alpha = 25, 50, 100$). It is also interesting to notice that these oscillations for absorbing particles become completely suppressed for angles $\theta > 50^\circ$. The broad maximum between 140° and 145° for water droplets which indicates the fogbow is not present for absorbing particles. It is also important to notice that for such large particles most of the total scattered light is scattered into the narrow forward direction of about zero to 2° , the intensities per unit solid angle being $\approx 10^3$ times the ones for back-scattering angles. This property is independent of the refractive index and the same for all α above 25. The physical explanation for this is that for large particles the diffraction of light occurs only in these very forward angles. For most measurements it cannot be distinguished from the direct light, and therefore the Q_s for such particles can be assumed as 1 instead of 2.

Absorption of Radiation by Carbon Particles Suspended in the Atmosphere

Before studying the absorption properties of a carbon-particle cloud, the optimum combination of particle number and size with respect to absorption for carbon particles must be found for a given total carbon mass.

The absorption coefficient of a particle cloud per unit volume is

$$j_a = N \cdot r^2 \pi Q_a(\alpha), \quad (8)$$

where N = number of particles per unit volume. If the volume of one particle is $V_p = 4\pi r^3/3$ and the total mass M of particles per unit volume is $V_t \cdot S$ (S = density), the number of particles per unit volume is $N = V_t \cdot 3/4 \pi r^3 = 3M_t/4 \pi r^3 \cdot S$. And j_a becomes

$$j_a = \frac{3}{4} \frac{M}{S} \frac{1}{r} Q_a(\alpha), \quad (9)$$

or with $r = \alpha \cdot \lambda / 2\pi$,

$$j_a = 3\pi \frac{M}{S} \frac{1}{2\lambda \cdot \alpha} Q_a(\alpha)$$

$$j_a = \text{const} \frac{1}{\alpha} Q_a(\alpha). \quad (10)$$

In Fig. 15, the function $Q_a(\alpha)/\alpha$ is plotted, and the graphical solution gives j_{\max} for $\alpha = 0.6$.

For sunlight with an intensity peak at $\lambda = 0.5$ micron, $\alpha = 0.6$ corresponds to $a = 0.05$ micron.

It should be mentioned here that carbon black of this size is commercially available; however, it is very likely that these small particles will form larger conglomerates during the dispersion process. Laboratory experiments on this problem will be necessary.

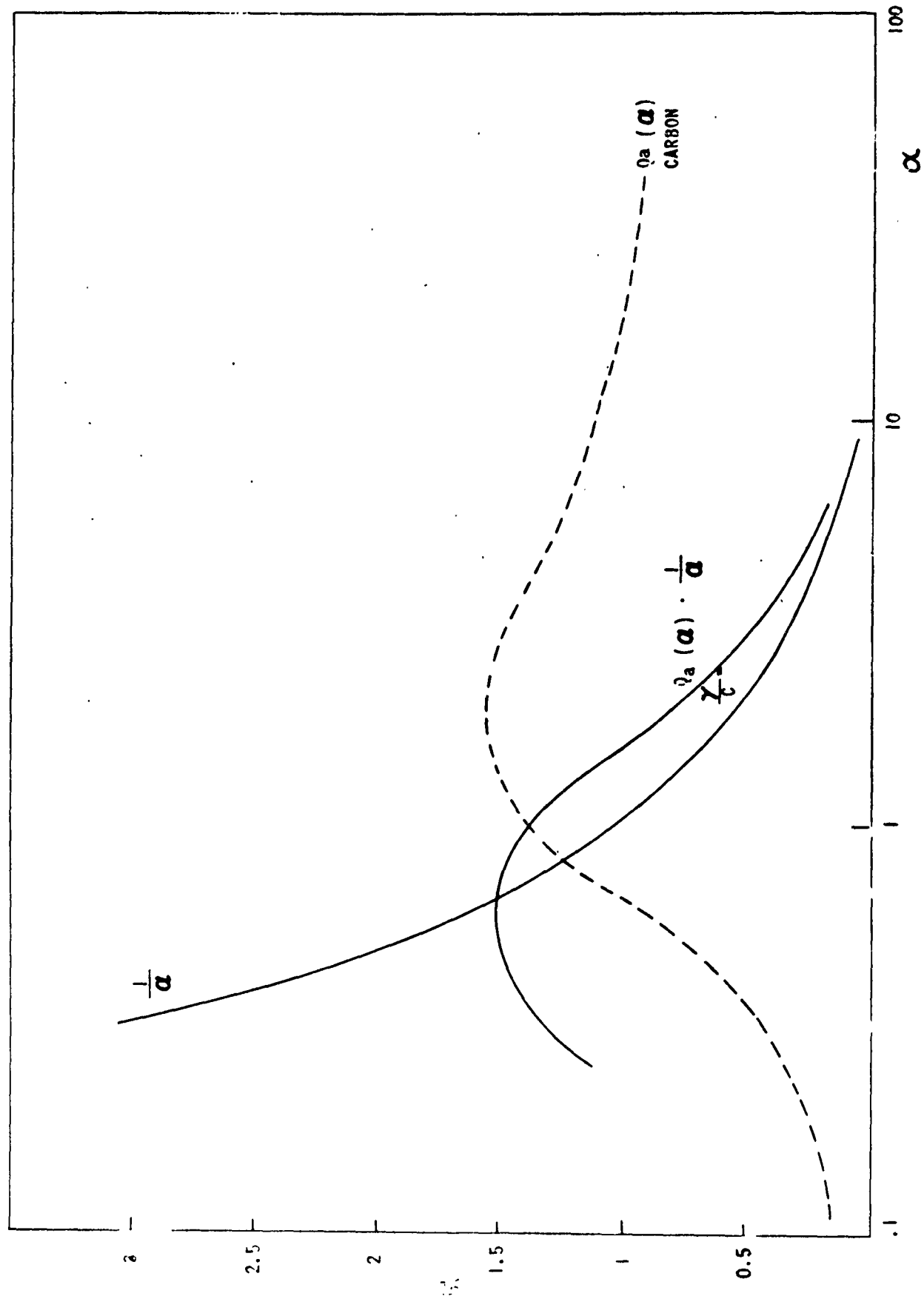


Fig. 15. Total absorption coefficient for a given total carbon mass per unit volume as a function of the size parameter.

After all necessary properties of single particles were investigated, a study of the processes of such particles in a cloud was begun. The following considerations and computations are based mainly on a thesis by G. Korb (1961, University of Munich, Germany) whose studies were carried out on Signal Corps Contract EUC-1612. The object of this study was to calculate the absorption, transmission, and reflection of radiation propagating through a cloud. In order to understand the significance of the results, a brief summary is given of Korb's solution.

In order to include multiple scattering effects in the cloud, a solution must be found for the general radiation transfer equation (Chandrasekhar¹¹). Korb's approach is to solve the equation for $2 + 2\pi$ radiation fluxes--one upward, one downward and 2π fluxes in the horizontal. This approximation reduces Chandrasekhar's equation to a system of linear differential equations whose solutions give the absorption, transmission, and reflection of radiation. The absorption is given as the amount of energy absorbed inside the cloud by particles and water vapor. The method also takes into consideration the absorption of radiation by water vapor above and below the cloud. These computations of the absorption, transmission, and reflection have to be carried out separately for narrow spectral bands of the sun spectrum (depending on the spectral dependence of the particle parameters), and eventually have to be added up to give the total values. If the albedo of the ground surface is $\neq 0$, the same procedure must be applied to so-called auxiliary fluxes, i.e., the diffuse radiation fluxes reflected from the ground surface; and the resulting absorption, transmission, and reflection of the primary and secondary fluxes must be added up.

The first part of Korb's study included the computation of absorption, transmission, and reflection for three model clouds of pure water droplets--a low cloud, a high cloud, and a cloud with large vertical extent.

Korb's method was applied here to calculate the absorption properties of a pure carbon particle cloud, a cloud mixed of droplets and carbon particles, and a cloud of compound concentric carbon-water droplets, all three clouds having a vertical extent of 1,000 meters, with their base near the ground surface:

(a) Pure carbon particle cloud. The carbon particle concentration is 10^4 particles per cm^3 , 0.1-micron-diameter size. This is equivalent to approximately 20 pounds of carbon black per 1 km^2 for a 1,000-meter-thick cloud. The water-vapor content in the cloud is assumed to be $2 \cdot 10^{-6} \text{ g/cm}^3$; the total water-vapor content above the cloud (above 850 mb) is 1.5 cm ppw (according to an average distribution over middle latitudes for summer, Korb, et al¹²).

(b) Mixed cloud. The cloud consists of droplets of 4 microns radius, $597/\text{cm}^3$, and 10^4 carbon particles/ cm^3 of 0.05 micron radius. The water-vapor content above the cloud is the same as before--1.5 cm ppw; the saturation water vapor density in the cloud is assumed to be $8 \cdot 10^{-6} \text{ g/cm}^3$ at about $+7.5^\circ\text{C}$, and the albedo of the ground is zero.

(c) Compound particle cloud. This is a cloud of particles which consists of a spherical carbon nucleus with a concentric water shell. The total particle size again is four microns radius and the concentration is

597/cm³. (This number results from a water content in the cloud of 0.16 g/m³.) All the carbon particles of the cloud in paragraph (a) will be inside the droplets, which gives 10,000/600 = 16.7 carbon particles/droplet. The size of the combined carbon-particle nucleus becomes approximately 0.125 micron radius, which gives a specific ratio b/a = 32. The water-vapor content in and above the cloud is the same as in paragraph (b).

The sun spectrum from 0.2 through 10 microns has been divided into 17 bands, and for each band the following quantities were computed:

$$k = \frac{K_a}{K_e} = \frac{\sum n \pi r^2 Q_a + S_w k_w (\lambda)}{\sum n \pi r^2 Q_e + S_w k_w (\lambda)} \quad (11)$$

and $T = \int K_e (\lambda) \cdot dh$, the optical density of the cloud. (12)

Then the intensity of sun radiation incident on the cloud, $E_0' (\lambda)$

was computed; and finally the absolute values of absorbed, transmitted, and reflected energy were obtained. All computations have been carried out for zenith distances of the sun of 0°, 30°, 60° and 80°.

The results of the computations are plotted in Fig. 16. In the graphs for a mixed cloud, the absorption curve for a pure water-droplet cloud (taken from Korb's report) has been added for comparison. Also added is the curve for E_0' , i.e., the intensity of energy incident on the cloud top after passing through the upper atmosphere. Approximately 0.2 · cal/cm² · min. are absorbed by water vapor in the upper atmosphere above the cloud, for vertical incidence. In the case of the pure carbon-particle cloud, the percentage of absorbed and transmitted energy is almost equal, with very little energy (< 5 percent) reflected back from the cloud top. For very-low sun elevations, such a cloud absorbs around 80 to 90 percent of the incident radiation, although the absolute amount of absorbed energy becomes very small for low sun elevations. If, as a comparison, the absorption in such a pure carbon cloud for single scattering only is calculated applying Bouguer's law,

$$E_a = E_0 \cdot (1 - e^{-\mathcal{K}_a \cdot L}), \quad (13)$$

substitution is made for $\mathcal{K}_a = N \cdot r^2 \pi Q_a = 5.5 \cdot 10^{-7} \text{ cm}^{-1}$, and the path length for zenith distance $z = 0$ is 10⁵ cm. Then, $E_a/E_0 = 5.5$ percent. The absorption by water vapor in the cloud is approximately 2.5 percent. This would give a total absorption of about 7 percent, only one-sixth of the actual absorption.

The optical properties of the mixed cloud are considerably different. About 60 percent of the incident radiation is reflected from such a cloud so that only a small portion of the radiation penetrates into the cloud. However, it can be seen that, because of the carbon particles, about three times more energy is absorbed than in the pure water-droplet cloud. Only about 12 percent of the incident light is transmitted through this cloud.

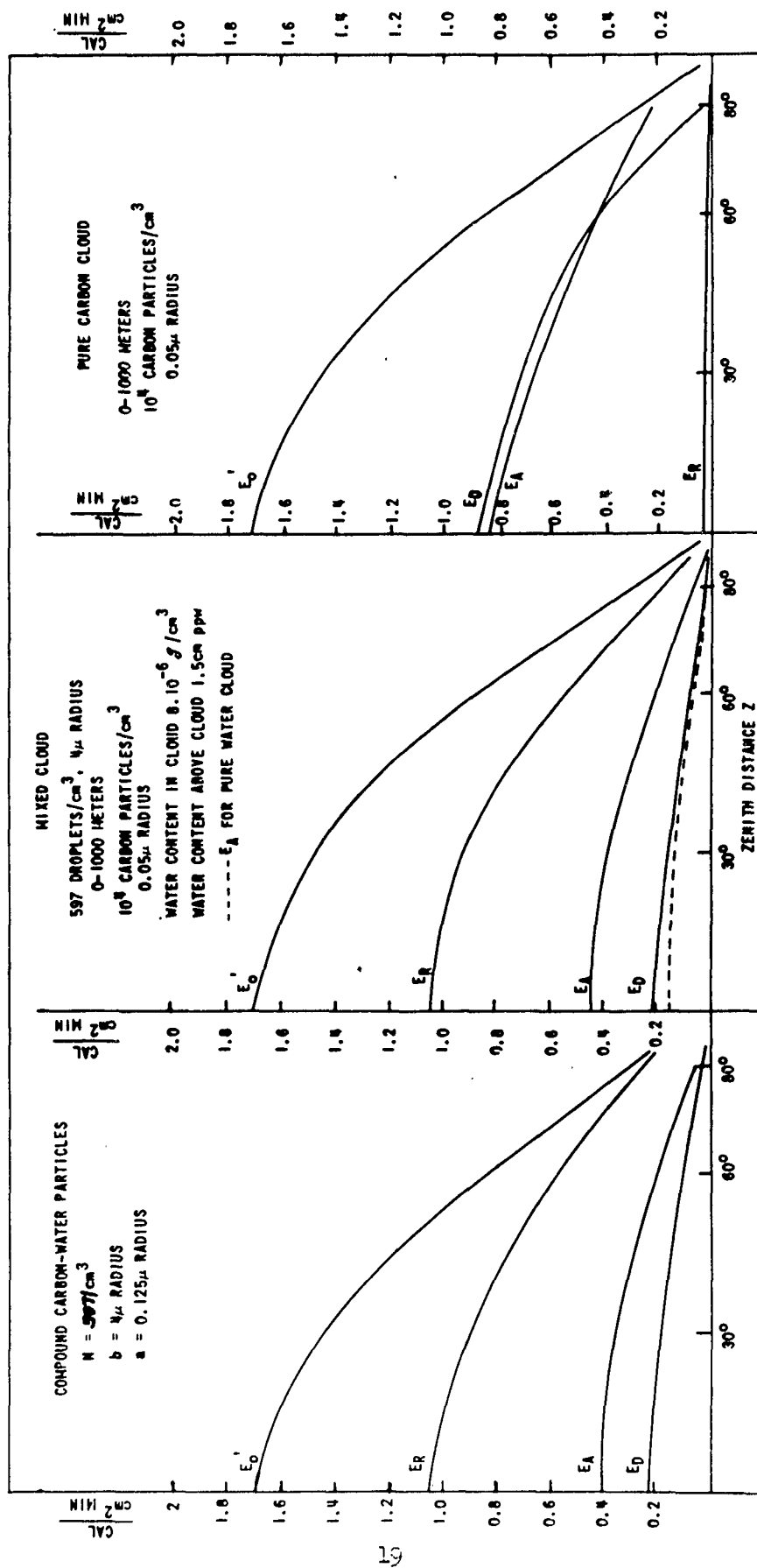


Fig. 16. Computed transmitted energy (E_D), absorbed energy (E_A) and reflected energy (E_R) for three cloud models, as function of sun zenith distance.

A very interesting result is that the optical properties of the mixed and the compound cloud are almost equal, the absorption of the mixed cloud being about 2 to 2.5 percent (of E_0') higher than for the compound particle cloud. From this it can be concluded that the form in which the carbon particles are distributed in the water-droplet cloud--whether they are in between the droplets, or inside, or on the surface--makes little difference in the absorption coefficient so long as the total carbon mass is about the same. This result is not too surprising if one looks at the spectral distribution of the absorbed energy. About 45 to 50 percent of the total absorbed energy is absorbed in the infrared between two and ten microns wavelength, although there is only about 27 percent of the total incident energy in this wavelength range. This is because of the high absorption of water in the infrared. This wavelength region is therefore influenced very little by the carbon absorption.

In the visible range, Figs. 10 and 11 show that for large b/a the absorption cross section $C_a = b^2 \pi \cdot Q_a$ remains rather constant and is only slightly higher than the one for the carbon nucleus without water shell. This result is important because it is not actually known what happens to the carbon particles in the cloud after seeding--whether they will attach themselves to the surface of droplets, or whether most of them will remain suspended in the air. It can be assumed that the rather special case of concentric compound particles will exist very seldom--probably only if condensation of water on the carbon particles occurs, most likely by radiational cooling of the carbon particles during nighttime.

So far in these calculations it has been assumed that the albedo of the ground surface is zero. This means that the upward-directed radiation flux at the bottom of the cloud is zero. The more light there is reflected from the ground back into the cloud, the higher the total absorption in the cloud will be. Korb has computed the absorption, transmission, and reflection of pure water-droplet clouds for various albedo values between zero and 0.9, and from his data it can be estimated that in the case of a mixed and compound particle cloud the absorption would be increased by about 2 to 3 percent (of E_0') if the ground albedo were 0.9 instead of zero. The increase in absorption is so small because, in addition to the ground-reflected radiation, a great percentage of radiation is reflected down from the bottom surface of the cloud. This increases the transmissivity of the cloud considerably. For the carbon particle cloud, of course, higher ground albedo would result in a much higher absorption. The denser a cloud, the less influence the ground albedo has on the absorption of the cloud.

For energy processes inside the cloud, the vertical distribution of the total absorbed energy within the cloud must be considered. From Korb's thesis it follows that for a cloud with optical thickness 30 km^{-1} (as in the compound and mixed-cloud model), for zenith distance $z = 30^\circ$ and ground albedo $A_g = 0$ and $K_a/K_e = 0.003$, 50 percent of the total absorbed radiation is absorbed in the upper 300 meters of the cloud; whereby, for $2 < \tau < 30$, the intensity of the downward-directed radiation flux almost follows a distribution of the form $E = -a\tau + b$. The denser the cloud, the greater the percentage of absorbed energy in the upper portion of the cloud.

If results of this study are compared with previous calculations by other investigators, the rather detailed study by Smith, et al.¹³ should be mentioned. They have computed the transmittance, reflectance, and absorption

of a mixed cloud of droplets and small absorbing particles, neglecting the absorption in droplets and applying the two-flux model by S. Fritz.¹¹ For high optical thicknesses the two-flux model gives about 10 percent lower transmission values, according to comparisons in Korb's report.¹² Using calculations of Smith, Wexler and Glasser,¹³ a cloud transmission of about 5 to 10 percent, and a reflectance of about 80 percent, a 10 to 15 percent absorption is obtained for the compound-particle cloud. This is for vertical incidence. Computations made under this study give about 25 percent absorption, 60 percent reflection, and 15 percent transmission. It seems that the two-flux model overemphasizes the reflectance of a cloud. For detailed discussions of the accuracy and significance of data obtained with the $2 + 2\pi$ flux model, reference is made to Korb's thesis.

Finally, an estimate is made of how much cloud evaporation or dissipation can be achieved with this absorbed energy. The radiation energy which is absorbed within the cloud is used for heating of the total air mass and water-droplet mass, and then for evaporation of the droplets. If it is assumed that the absorption and evaporation process occurs slowly enough so that equilibrium conditions are close between all the components and the atmosphere, then, for the energy budget,

$$dq = c_{pa} \cdot \rho_a \cdot dT + c_w \cdot w \cdot \rho_w \cdot dT + L \cdot w. \quad (14)$$

c_{pa} = specific heat of air for const. pressure, 0.24 cal/g °C

ρ_a = density of air, at 7.5° and 90° mb = 1.12 g/cm³

c_w, ρ_w = spec. heat and density of water;

w = liquid water content of cloud g/m³,

L = latent heat of vaporization of water, 590 cal/g °C.

Substituting these values into equation (14),

$$\begin{aligned} dq &= 269 + 0.155 + 87 \text{ (cal/m}^3\text{)} \\ &= 356 \text{ cal/m}^3 \text{ for a } 1^\circ\text{C temperature increase.} \end{aligned}$$

Heating of the carbon particles has been neglected completely because their mass is only about 1/100,000th of the water content and it is seen that even the energy required for the heating of the droplets is negligible. The temperature rise which is required to increase the saturation water vapor content from the original 8 g/m³ to 8.15 g/m³ is approximately 0.3°C. From equation (14), therefore, is obtained the energy required to evaporate the compound-particle cloud and to achieve the necessary temperature increase of 0.3°C to about 100 cal/m³.

In the case of the mixed cloud and the compound-particle cloud, the absorbed energy for sun zenith distances between zero and 30° is about 0.4 cal/cm² min. The air column below 1 cm² is $1 \cdot 10^5 \text{ cm}^3 = 0.1 \text{ m}^3$, which gives an average absorbed energy of 4 cal/m³ · min. This would result in a necessary absorption time of about 25 minutes. For a sun zenith distance of 60°, the absorbed energy would be only about 0.2 cal/cm² min. and the absorption time therefore twice as long--approximately 50 minutes.

Actually, it must be expected that the upper 100 meters of the cloud, where the absorption per unit volume is about twice the average absorption, will start to warm up and evaporate first. This will, again, allow more radiation to penetrate into the lower layers of the cloud. However, as soon as the upper layer starts to warm up it will also begin to rise and cool off again. It certainly will be necessary to provide more than the minimum energy for a 0.3°C temperature increase if the evaporation process is to be maintained long enough to evaporate the cloud completely.

Van Straten⁵ suggested as a hypothetical process for the cloud dissipation an evaporation and condensation process between droplets. Droplets containing many carbon particles would heat up more than pure water droplets, and therefore moisture would evaporate from the warmer droplets with the carbon particles onto the colder pure water droplets.

A droplet containing carbon particles will absorb energy and consequently its temperature will rise. This again will cause an energy loss by conduction and evaporation. The energy budget can be written in the following way:

$$\frac{dE_a}{dt} = c \cdot m \cdot \frac{dT}{dt} + 4\pi r \cdot K \cdot (T - T_0) + 4\pi r^2 \cdot \rho \cdot L \frac{dr}{dt} \quad (15)$$

c = specific heat of water = $1 \text{ cal. degr.}^{-1} \cdot \text{g}^{-1}$

m = mass of droplet

r = droplet radius

K = thermal conductivity of air = $5 \cdot 8 \cdot 10^{-5} \text{ cal. cm}^{-1} \cdot \text{sec}^{-1} \cdot \text{degr}^{-1}$

T = droplet temperature

T_0 = air temperature

ρ = water density = 1 g. cm^{-3}

L = latent heat of evaporation = $590 \text{ cal. g}^{-1} \cdot \text{degr}^{-1}$

$$\text{whereby } \frac{dr}{dt} = \frac{D}{\rho \cdot r} (\rho_d - \rho_w) \quad (16)$$

D = coefficient of diffusion of water vapor = $0.226 \text{ cm}^2 \cdot \text{sec}^{-1}$

ρ_d, ρ_w = vapor density of water at the droplet surface and far away from the droplet, respectively.

ρ_d is a function of T and r , according to Kelvin's formula:

$$\rho_d = \frac{M}{R \cdot T} \cdot p_w(T) \cdot \exp\left(\frac{2\sigma M}{R \cdot r \cdot T}\right) \quad (17)$$

σ = specific surface energy of water = $74.5 \text{ cal. cm}^{-2}$

M = molecular weight of water = 18

R = universal gas constant = $1.98 \text{ cal. g}^{-1} \cdot \text{degr}^{-1}$.

Substituting (16) and (17) in (15),

$$\frac{dE_a}{dt} = c \cdot m \cdot \frac{dT}{dt} + 4\pi r \cdot K(T - T_0) + 4\pi r L D \left[\left(\frac{\rho_w(T)}{\rho_w(T_0)} \right) \cdot \exp\left(\frac{2\sigma M}{RrT}\right) - 1 \right] \quad (18)$$

As a first approximation, it is assumed that r is constant and the following abbreviations are used:

$$\alpha = c \cdot m = 2.68 \cdot 10^{-10} \text{ cal} \cdot \text{degr}^{-1}$$

$$\beta = 4 \pi r K = 2.96 \cdot 10^{-7} \text{ cal} \cdot \text{degr}^{-1} \cdot \text{sec}^{-1}$$

$$\gamma = 4 \pi r L D = 0.67 \text{ cal g cm}^{-3} \text{ sec}^{-1}$$

$$\delta = \frac{2 \sigma M}{R \cdot r} = 0.082 \text{ degr.}$$

$$\frac{dE_a}{dt} = q = \frac{r^2 \pi \cdot Q_a \cdot E_0}{60} = 215 \cdot 10^{-11} \text{ cal} \cdot \text{sec}^{-1}$$

with $Q_a = 0.002$, $E_0 = 1.5 \text{ cal} \cdot \text{cm}^{-2} \cdot \text{min}^{-1}$.

We then get

$$q = \alpha \frac{dT}{dt} + \beta (T - T_0) + \gamma \left\{ S_w(T) e^{\frac{\delta}{T}} - S_w(T_0) \right\},$$

$$\text{or } \alpha \frac{dT}{dt} + \beta T + \gamma S_w(T) e^{\frac{\delta}{T}} = q + \beta T_0 + \gamma S_w(T_0) \quad (20)$$

$c = q + \beta T_0 + \gamma S_w(T_0)$ is constant. The magnitude of each of the three quantities ($q = 2.5 \cdot 10^{-11}$, $\beta T_0 = 8 \cdot 3 \cdot 10^{-5}$, and $\gamma \cdot S_w(T_0) = 5.4 \cdot 10^{-6}$), shows that q will have to be 100,000 times bigger to be of any influence on the result of this equation. This confirms Smith, Wexler, and Glaser's conclusion¹³ that 10^4 particles per droplet would be necessary to achieve a sufficient rise of temperature in the droplet.

An analytical integration of equation (18) will be extremely difficult, if not impossible. However, since in this study there is not much interest in the transient phase, $dT/dt = 0$ is assumed and T is calculated only after reaching equilibrium conditions.

$$\beta T + \gamma S_w(T) e^{\frac{\delta}{T}} - c = 0. \quad (21)$$

The numerical solution gives $T = 280.46^\circ \text{K}$ or 7.3°C . The temperature of the particle has decreased by 0.2°C from the initial temperature, $T_0 = T_{\text{air}}$. From an assumed air temperature of 7.5°C , evaporation due to the curvature of the droplet was obtained. Also, from equation (18), it can be seen that the condensation term is of the order 10^{-7} and the evaporation term is of the order 10^{-6} ; and the first term, the internal energy increase, is of an order $< 10^{-10}$, which means that most of the absorbed energy is lost by conduction to the surrounding air. This loss of energy to the air will actually be even greater since the heat transfer does not occur only by conduction but also by convection. Consequently, the air temperature will rise almost as fast as the particle temperature. It has been shown that for small absorption rates the particle temperature may be even below the air temperature because of evaporation due to vapor-pressure difference. Most of the

evaporated water from the droplets will be needed to maintain saturation in the heated air, and only a very small portion would be available for condensation on pure droplets. Therefore, it can be stated definitely that an evaporation-condensation process cannot be considered as a possible cloud-dissipation process, and therefore the only possible dissipation process for carbon-seeded clouds will be evaporation due to heating of the total air mass which, as has been shown, requires very large quantities of carbon black.

This report has been limited to absorption processes only, and no discussion has been made of any emission effects from carbon seeded clouds. For more information on the energy budget in clouds, a study is certainly necessary. As a result of the very encouraging results of the first part of Korb's study and the results reported here, the studies by the University of Munich, Germany, have been extended under Signal Corps contract to also cover various models of pure and mixed carbon and water clouds to a much higher extent and accuracy than has been done in work reported here. This extended study will also include energy losses due to emission from the cloud.

CONCLUSIONS

A summary of the results indicates that for a model cloud of approximately 600 droplets/cm³, 4 micron radius, from ground to 1,000 meters altitude (stratus-type cloud), seeding with 20 pounds of 0.05 micron radius carbon particles will increase the absorption of sun radiation within the cloud from about 0.15 to 0.4 cal/cm² · min for 0° to 30° sun zenith distance.

The absorption, transmission and reflection are almost equal for a mixed cloud of water droplets and carbon particles and a cloud of compound concentric carbon-water particles. This indicates very strongly that for absorption studies it is not very critical to know in what form the carbon particles are distributed within the cloud, i.e., whether they are contained within the cloud droplet or attached to its surface.

From estimates of the energy required for evaporation of the model cloud it is concluded that for realistic field experiments it will be necessary to use seeding rates of the order of at least 100 pounds of carbon black per km² during high sun elevations and for relatively stable cloud formations. The necessary seeding rate may go up to several hundred pounds per km² under less favorable conditions.

An analysis of the energy budget in the seeded cloud yields that an evaporation-condensation process will not be possible, and that evaporation of a cloud due to heating of the total air mass will be possible only under very favorable conditions.

REFERENCES

1. Schaefer, V. J., Science, 104, p 457 (1946).
2. Vonnegut, B., Jour. Appl. Phys., 18, p 593 (1947).
3. Findeisen, W., Met. Z. 55, p 121 (1938).

4. Mie, G., Ann. Physik, 25, p 377 (1908).
5. Van Straten, F., R. Ruskin, J. Dinger, H. Mastenbrook, NRL Rpt. 5235 (1958).
6. Aden, A. L. and M. L. Kerker, Jour. Appl. Phys. 22, p 1242 (1951).
7. Shifrin, K. S., Doklady AN SSSR, Nowaya Seriya 94, No. 4 (1954).
8. Dietrich, G., Ann. d. Hydrogr., 67, p 411 (1939).
9. Van De Hulst, Light Scattering by Small Particles, John Wiley, New York (1957).
10. Giese, R. H., Met. Rundschau (1961).
11. Chandrasekhar, S., Radiative Transfer, Oxford Univ. Press (1950).
12. Korb, G., J. Michalowsky, and F. Möeller, Tech. Rpt. No. 2, Contract AF 61(514)-1005 (1957).
13. Smith, R., R. Wexler, and A. Glaser, Final Rpt, Contract AF 19 (604)-3492 (1959).
14. Fritz, S., Jour. Met. Vol. 11, pp 291-300 (1954).

DISTRIBUTION

No. of Copies

Chief Signal Officer, ATTN: SIGRD Department of the Army, Washington 25, D. C.	1
Chief Signal Officer, ATTN: SIGPD-8b1 Department of the Army, Washington 25, D. C.	2
Office of the Assistant Secretary of Defense (Research and Engineering), ATTN: Technical Library Room 3E1065, The Pentagon, Washington 25, D. C.	1
Chief of Research and Development Department of the Army, Washington 25, D. C.	2
Chief, United States Army Security Agency ATTN: ACofS, G4 (Technical Library) Arlington Hall Station, Arlington 12, Virginia	1
Commanding General, U. S. Army Electronic Proving Ground ATTN: Technical Library, Fort Huachuca, Arizona	1
Commanding Officer, ATTN: SIGWS-AJ U. S. Army Signal Missile Support Agency White Sands Missile Range, New Mexico	1
Commanding Officer, ATTN: SIGMS-ADJ U. S. Army Signal Materiel Support Agency Fort Monmouth, New Jersey	1
Directorate of Intelligence, ATTN: AFOIN-1b1 Headquarters, U. S. Air Force, Washington 25, D. C.	2
Commander, ATTN: RAALD, Rome Air Development Center Griffiss Air Force Base, New York	1
Commanding General, ATTN: ROZMS Hq, Ground Electronics Engineering Installations Agency Griffiss Air Force Base, New York	1
Commander, ATTN: ASAPRL, Aeronautical Systems Division Wright-Patterson Air Force Base, Ohio	1
Commander, U. S. Air Force Security Service ATTN: Directorate of Systems Engineering (DSD) DCS/Communications-Electronics San Antonio, Texas	1
Commander-in-Chief, ATTN: DOCER, Strategic Air Command Offutt Air Force Base, Nebraska	1
Commander, Air Proving Ground Center, ATTN: PGAPI Eglin Air Force Base, Florida	1

DISTRIBUTION (cont)

No. of Copies

Commander, Air Force Cambridge Research Laboratories ATTN: CRO, Laurence G. Hanscom Field Bedford, Massachusetts	2
Commander, Air Force Electronic Systems Division ATTN: CCRR and CCSD, Laurence G. Hanscom Field Bedford, Massachusetts	2
Commander, Air Weather Service (MATS), U. S. Air Force ATTN: AWSSS/TIPD, Scott Air Force Base, Illinois	1
AFSC Liaison Office Naval Air Research and Development Activities Command Johnsville, Pennsylvania	1
Chief of Naval Research, ATTN: Code 427 Department of the Navy, Washington 25, D. C.	1
Bureau of Ships Technical Library, ATTN: Code 312 Main Navy Building, Room 1528, Washington 25, D. C.	1
Chief, Bureau of Ships, ATTN: Code 454 Department of the Navy, Washington 25, D. C.	1
Chief, Bureau of Ships, ATTN: Code 686B Department of the Navy, Washington 25, D. C.	1
Director, ATTN: Code 2027 U. S. Naval Research Laboratory, Washington 25, D. C.	1
Commanding Officer and Director, ATTN: Library U. S. Navy Electronics Laboratory San Diego 52, California	1
Commander, U. S. Naval Ordnance Laboratory White Oak, Silver Spring 19, Maryland	1
Director, ATTN: Technical Documents Center U. S. Army Engineer Research and Development Laboratories Fort Belvoir, Virginia	1
Commanding Officer, ATTN: Technical Library, Building 330 U. S. Army Chemical Warfare Laboratories Army Chemical Center, Maryland	1
Commander, Armed Services Technical Information Agency ATTN: TIPCR, Arlington Hall Station, Arlington 12, Virginia	10
Signal Corps Liaison Officer, Ordnance Tank Automotive Command U. S. Army Ordnance Arsenal, Detroit, Center Line, Michigan	1

DISTRIBUTION (cont)

No. of Copies

Army Liaison Officer, ATTN: Code 1071 Naval Research Laboratory, Washington 25, D. C.	1
Signal Corps Liaison Officer, Mass. Institute of Technology Building 26, Room 131, 77 Massachusetts Avenue Cambridge 39, Massachusetts	1
U. S. Army Signal Liaison Office, ATTN: ASDL-9 Aeronautical Systems Division Wright-Patterson Air Force Base, Ohio	2
Signal Corps Liaison Officer, Lincoln Laboratory P. O. Box 73, Lexington, Massachusetts	1
Signal Corps Liaison Officer, Rome Air Development Center ATTN: RAOL, Griffiss Air Force Base, New York	1
Liaison Officer, Los Angeles Area U. S. Army Signal R and D Laboratory 75 South Grand Avenue, Building 13, Pasadena, California	1
USASRDL Liaison Officer, Hq, U. S. Continental Army Command Fort Monroe, Virginia	1
USASIMSA Liaison Engineer, Signal Section Eighth U. S. Army, A.P.O. 301, San Francisco, California	1
Chief Scientist, SIGRA/SL-CS, Hq, USASRDL	1
USASMSA Liaison Office, SIGRA/SL-LNW, USASRDL	1
Corps of Engineers Liaison Officer, SIGRA/SL-LNE, USASRDL	1
Marine Corps Liaison Officer, SIGRA/SL-LNR, USASRDL	1
U. S. CONARC Liaison Officer, SIGRA/SL-LNF, USASRDL	3
Commanding Officer, U. S. Army Signal Research Activity Evans Area	1
Chief, Technical Information Division, Hq, USASRDL	6
USASRDL Technical Documents Center, Evans Area	1
Mail File and Records, File Unit No. 3, Evans Area	1
U. S. Army Research Office, Research Analysis Division ATTN: Dr. Hoyt Lemons, Arlington Hall Station, Virginia	1
Commanding General, U. S. Army Electronic Proving Ground ATTN: Meteorological Department, Fort Huachuca, Arizona	1

DISTRIBUTION (cont)

	No. of Copies
Commanding General, U. S. Army Electronic Proving Ground ATTN: SIGPG-DCGM, Fort Huachuca, Arizona	2
Chairman, U. S. Army Chemical Corps Meteorological Committee Fort Detrick, Frederick, Maryland	1
Director, U. S. Army Chemical Corps Operations Research Group, Army Chemical Center, Edgewood, Maryland	1
Director, Atmospheric Sciences Program National Science Foundation, Washington 25, D. C.	1
Director, Bureau of Research and Development Federal Aviation Agency National Aviation Facilities Experimental Center ATTN: Technical Library, Bldg. 3, Atlantic City, New Jersey	1
Chief, Fallout Studies Branch, Division of Biology and Medicine, Atomic Energy Commission, Washington 25, D. C.	1
Chief, Bureau of Naval Weapons (FAME) U. S. Navy Department, Washington 25, D. C.	1
Officer-in-Charge, Meteorological Curriculum U. S. Naval Post Graduate School, Monterey, California	1
Chief of Naval Operations (OP07) U. S. Navy Department, Washington 25, D. C.	1
Office of Naval Research, U. S. Navy Department Washington 25, D. C.	1
U. S. Naval Research Laboratory, ATTN: Code 7110 Washington 25, D. C.	1
Marshall Space Flight Center, Aeroballistic Division Aerophysics Branch (Aero-G), ATTN: William Vaughn Huntsville, Alabama	1
Office of U. S. Naval Weather Service U. S. Naval Air Station, Washington 25, D. C.	1
Officer-in-Charge, U. S. Naval Weather Research Facility U. S. Naval Air Station, Norfolk, Virginia	1
U. S. Army Corps of Engineers Snow, Ice, and Permafrost Research Establishment 1215 Washington Avenue, Wilmette, Illinois	1
U. S. Army Corps of Engineers, Waterways Experiment Station Vicksburg, Mississippi	1

DISTRIBUTION (cont)

No. of Copies

Office of the Chief of Ordnance, Department of the Army Washington 25, D. C.	1
Chief, Aerophysics Branch, Aeroballistics Laboratory Army Ballistic Missile Agency, Redstone Arsenal, Alabama	1
Commanding Officer, ATTN: Technical Information Section Picatinny Arsenal, Dover, New Jersey	1
Chief, Meteorological Division, U. S. Army Chemical Corps Proving Ground, Dugway Proving Ground, Utah	1
Director, Meteorological Division, Surveillance Department	1
Chief, Atmospheric Physics Branch, Meteorological Division	25
Chief, Meteorological Systems Branch, Meteorological Division	1
Chief, Meteorological Instrumentation Branch, Meteorological Division	1
Technical Reports Unit, Meteorological Division	1
Chief, Bureau of Naval Weapons, U. S. Navy Department ATTN: Dr. E. F. Corwin, Washington 25, D. C.	1
Commander, Air Force Electronic Systems Division Geophysics Research Directorate, ATTN: Dr. R. Cunningham L. G. Hanscom Field, New Bedford, Massachusetts	1
U. S. Naval Research Laboratory, ATTN: Dr. J. E. Dinger Washington 25, D. C.	1
Director, Atmospheric Sciences Program, National Science Foundation, Washington 25, D. C., ATTN: Dr. Earl Droessler	1
Director, Bureau of Research and Development Federal Aviation Agency, National Aviation Facilities Experimental Center, Atlantic City, New Jersey ATTN: Mr. A. Hilsenrod	1
U. S. Weather Bureau, Washington 25, D. C. ATTN: Mr. Dwight Kline	1
New Mexico Institute of Mining and Technology, Socorro, New Mexico, ATTN: Dr. E. J. Workman	1

AD	Div	UNCLASSIFIED	AD	Div	UNCLASSIFIED
Army Signal Research and Development Laboratory, Fort Monmouth, New Jersey		1. Weather Modification 2. Light-scattering and Absorption	Army Signal Research and Development Laboratory, Fort Monmouth, New Jersey		1. Weather Modification 2. Light-scattering and Absorption
THEORETICAL CONSIDERATIONS ON THE EFFECTIVENESS OF CARBON SEEDING by Robert Fenn and Hansjörg Oser, March 1962, 25p. incl. illus. table, 14 refs. (USASRD Technical Report 2258) (DA Task 3A99-27-005-03) Unclassified Report		I. Fenn, Robert Oser, Hansjörg	THEORETICAL CONSIDERATIONS ON THE EFFECTIVENESS OF CARBON SEEDING by Robert Fenn and Hansjörg Oser, March 1962, 25p. incl. illus. table, 14 refs. (USASRD Technical Report 2258) (DA Task 3A99-27-005-03) Unclassified Report		I. Fenn, Robert Oser, Hansjörg
Presented in the report are: some results of machine computations of the scattering functions, the extinction-, scattering-, and absorption-coefficients for pure absorbing carbon particles, and the compound carbon particles with concentric water shell of varying thickness; and an analysis of the absorption properties of various single particles.		II. Army Signal Research and Development Laboratory, Fort Monmouth, N. J.	Presented in the report are: some results of machine computations of the scattering functions, the extinction-, scattering-, and absorption-coefficients for pure absorbing carbon particles, and the compound carbon particles with concentric water shell of varying thickness; and an analysis of the absorption properties of various single particles.		II. Army Signal Research and Development Laboratory, Fort Monmouth, N. J.
		III. DA Proj. 3A99-27-005-03			III. DA Proj. 3A99-27-005-03
UNCLASSIFIED			UNCLASSIFIED		
The scattering and absorption properties of single particles are used to calculate the absorptivity, transmissivity, and reflectivity of three			The scattering and absorption properties of single particles are used to calculate the absorptivity, transmissivity, and reflectivity of three		
	(over)			(over)	
AD	Div	UNCLASSIFIED	AD	Div	UNCLASSIFIED
Army Signal Research and Development Laboratory, Fort Monmouth, New Jersey		1. Weather Modification 2. Light-scattering and Absorption	Army Signal Research and Development Laboratory, Fort Monmouth, New Jersey		1. Weather Modification 2. Light-scattering and Absorption
THEORETICAL CONSIDERATIONS ON THE EFFECTIVENESS OF CARBON SEEDING by Robert Fenn and Hansjörg Oser, March 1962, 25p. incl. illus. table, 14 refs. (USASRD Technical Report 2258) (DA Task 3A99-27-005-03) Unclassified Report		I. Fenn, Robert Oser, Hansjörg	THEORETICAL CONSIDERATIONS ON THE EFFECTIVENESS OF CARBON SEEDING by Robert Fenn and Hansjörg Oser, March 1962, 25p. incl. illus. table, 14 refs. (USASRD Technical Report 2258) (DA Task 3A99-27-005-03) Unclassified Report		I. Fenn, Robert Oser, Hansjörg
Presented in the report are: some results of machine computations of the scattering functions, the extinction-, scattering-, and absorption-coefficients for pure absorbing carbon particles, and the compound carbon particles with concentric water shell of varying thickness; and an analysis of the absorption properties of various single particles.		II. Army Signal Research and Development Laboratory, Fort Monmouth, N. J.	Presented in the report are: some results of machine computations of the scattering functions, the extinction-, scattering-, and absorption-coefficients for pure absorbing carbon particles, and the compound carbon particles with concentric water shell of varying thickness; and an analysis of the absorption properties of various single particles.		II. Army Signal Research and Development Laboratory, Fort Monmouth, N. J.
		III. DA Proj. 3A99-27-005-03			III. DA Proj. 3A99-27-005-03
UNCLASSIFIED			UNCLASSIFIED		
The scattering and absorption properties of single particles are used to calculate the absorptivity, transmissivity, and reflectivity of three			The scattering and absorption properties of single particles are used to calculate the absorptivity, transmissivity, and reflectivity of three		
	(over)			(over)	

cloud models: a pure carbon particle cloud, a cloud of water droplets and carbon particles, and a cloud of compound concentric carbon-water particles. All three clouds are 1,000 meters thick and near the ground.

The temperature change of one particle caused by radiation absorption has been computed, and the total energy for evaporation of a cloud mass has been estimated.

From these calculations it can be concluded that a total carbon mass of the order of several hundred pounds per km^2 will be necessary to evaporate a stratus-type cloud.

Unclassified Report

cloud models: a pure carbon particle cloud, a cloud of water droplets and carbon particles, and a cloud of compound concentric carbon-water particles. All three clouds are 1,000 meters thick and near the ground.

The temperature change of one particle caused by radiation absorption has been computed, and the total energy for evaporation of a cloud mass has been estimated.

From these calculations it can be concluded that a total carbon mass of the order of several hundred pounds per km^2 will be necessary to evaporate a stratus-type cloud.

Unclassified Report

cloud models: a pure carbon particle cloud, a cloud of water droplets and carbon particles, and a cloud of compound concentric carbon-water particles. All three clouds are 1,000 meters thick and near the ground.

The temperature change of one particle caused by radiation absorption has been computed, and the total energy for evaporation of a cloud mass has been estimated.

From these calculations it can be concluded that a total carbon mass of the order of several hundred pounds per km^2 will be necessary to evaporate a stratus-type cloud.

Unclassified Report

cloud models: a pure carbon particle cloud, a cloud of water droplets and carbon particles, and a cloud of compound concentric carbon-water particles. All three clouds are 1,000 meters thick and near the ground.

The temperature change of one particle caused by radiation absorption has been computed, and the total energy for evaporation of a cloud mass has been estimated.

From these calculations it can be concluded that a total carbon mass of the order of several hundred pounds per km^2 will be necessary to evaporate a stratus-type cloud.

Unclassified Report